Analysis of borehole breakout development using continuum damage mechanics

Author links open overlay panel David P.Sahara[ab] MartinSchoenball[c] EleniGerolymatou[d] ThomasKohl[a]
Show more

https://doi.org/10.1016/j.ijrmms.2017.04.005Get rights and content

Highlights

- Implementation of CDM concept to model breakout in an elastoplastic material
- Reproduce key characteristics of the transient failure as observed in experimental tests
- A good agreement between our numerical model and experimental tests
- Relation between the magnitude of the far field stresses and the size of breakouts

Abstract

Damage distribution and evolution have a significant effect on borehole stress concentrations. To model the complex fracturing process and inelastic deformation in the development of the borehole breakout, we implement a continuum damage mechanics (CDM) concept that takes tensile and compressive failure mechanisms into account. The proposed approach explicitly models the dissipative behavior of the material due to crackingand its evolution, which leads to an inhomogeneous redistribution of material properties and stresses in the vicinity of the borehole wall. We apply a constitutive plastic model for Berea sandstone and compare our numerical results to laboratory experiments performed on Tablerock sandstone. We are able to reproduce several characteristics of the failure process during the breakout development as observed in experimental tests, e.g. localized crack distribution in the vicinity of the borehole wall, damage evolution, which exhibits a widening process in the beginning followed by subsequent growth in depth, and shear fracturing-dominated breakout growth in sandstone. A comparison of our results with laboratory experiments

performed on a range of stress conditions shows a good agreement of the size of borehole breakouts. The importance of the constitutive damage law in defining the failure mechanisms of the damaging processes is discussed. We show that the depth and the width of breakouts are not independent of each other and no single linear relation can be found between the size of breakouts and the magnitude of the applied stress. Consequently, only one far field principal stress component can be estimated from breakout geometry, if the other two principal stresses are known and sufficient data on the plastic parameters are available.

- **Previous** article in issue
- **Next** article in issue

Keywords

Damage mechanics
Borehole breakout development
Failure mechanism
Elastic and plastic deformation
Fracturing process

1. Introduction

Continuum damage mechanics (CDM) was developed based on the work of Kachanov[1] and Rabotnov,[2] who considered the creep of metal. In this concept, the progressive material damage is used to explain distributed defects in the material and structure that lead to crack initiation and coalescence to fractures. The theoretical framework was not developed further until the work of Chaboche[3] who used the general framework of thermodynamics of irreversible processes. The CDM approach does not prescribe the microcracks that cause the damage, rather it uses a damage parameter to define the effect of damage on the free energy of the system.[4] CDM has been successfully applied to model the failure process in a wide range of materials, e.g. steel,[5] concrete,[6] ceramics[7] and others. One of the success factors of this approach stems from the use of a single constitutive model that governs the nonlinear behavior of the material including failure, both in tension and compression.[8]

Modeling the expected degree of damage of a rock mass around cavities is required in many subsurface geotechnical problems such as boreholes and tunnels. The importance of the material properties on the borehole breakout development have been highlighted in some studies, e.g. Zheng et al.,[9] Sahara et al.[10] among many others. Several modeling attempts, that take into account the changes of the material properties

of the rock, have been conducted in order to model the damage propagation around boreholes. Cheatham[11] modeled the damage zone around the borehole as a soft inclusion and found that the residual stiffness in soft zones developing due to the damage is sufficient to alter the stress concentration. Nawrocki and Dusseault[12] modeled the damage zone by introducing a radius-dependent Young's modulus around the borehole wall, and calculated the corresponding stress distribution around the borehole. Detournay[13] further developed the concept for a plastic material. Gaede et al.[14] incorporated anisotropy in a non-linear plastic model. Schoenball et al.[15] analyzed time-dependent breakout formation with a simplified damage mechanics approach. Previous laboratory experiments on borehole breakouts have shown that failure of the borehole wall is often governed by two different modes: tensile spalling and shear fracturing.[16], [17] Laboratory experiments can be used to study the micromechanical failure of boreholes from the condition of breakouts at the end of an experiment. However, it is difficult to explain the failure processes that lead to the final breakout shape. CDM has led to considerable progress in understanding the onset, development and stabilization of failure. It typically requires extensive testing to determine the relevant constitutive damage laws as well as the strength and yielding criteria. Busetti et al.[18] developed a CDM model to describe the progressive damage accumulation that finally leads to brittle failure in Berea sandstone. Uniaxial and triaxial tests were performed to calibrate the model. It was found that the damage and fracturing patterns simulated by the CDM match the experimental features very well.

Herein, we intend to demonstrate that CDM is able to characterize key observations of the transient development of borehole breakouts in an elastoplastic material. Our investigation allows us to account for both tensile and compressive failure. We use the single constitutive law by Lee and Fenves[8] in our modeling scheme. The damage law obtained by Busetti et al.[18] is used as a basis for the non-linear deformation involved in the simulation. A sensitivity study is performed to analyze the significance of each parameter possibly affecting the dimensions of borehole breakouts. We compare our results to available experimental data from Ewy,[19] Haimson and Lee,[20] Haimson.[21] In general, a good match between modeling and laboratory experiment results is achieved.

2. Theoretical framework

2.1. Fracturing and damage

The failure of most rock materials is a process of crack initiation and propagation. A number of approaches to model those phenomena have been proposed in the past.

Many of them were formulated for a linear elastic medium, e.g. fracture mechanics based on the Griffith theory.[22] Fracture mechanics assume that a fracture grows from a small initial crack that amplifies the local stresses at the crack tip and the fracture propagates when the local stresses exceed the strength of the material. Fracture mechanics assesses the strength of a stressed material through the relationship between the loading conditions, the geometry of the crack and the resistance to crack propagation in terms of strain energy release rate (G) or stress intensity factor (K). In this approach the propagation of the fracture is modeled either by cohesive crack tip[23] or a shielding zone.[24] This model is relevant for fracture propagation in rocks that exhibit macroscopic propagation via coalescence of microcracks within a damage front. However the rock stiffness degradation due to the increase of microcrack density[25, 26] cannot be modeled with fracture mechanics. Furthermore, as experiments show, there exist inelastic deformations around the crack front which contradict the assumption of a linear elastic medium.[27] These inelastic deformations could be modeled by taking into account the plasticity in the modeling scheme, i.e. the strain hardening/softening phase due to the accumulation of microcracking .[28] Macroscopically, this degraded stiffness is linked to the evolution of stress-induced damage that leads to local fracturing and, eventually, to failure.[29]
A continuum damage mechanics concept is used in this study to handle the complex material failure process and the inelastic deformation that cannot be explained by the elastic approach. With this concept the deformation of the material is simulated, based on the damage evolution due to microcrack development, which might better represent the in-situ rock behavior. Unlike the insertion of cohesive or shielding zones, damage propagation is localized within weakening zones that are determined by the plastic deformation. Yielding is characterized by nonlinear inelasticity associated with stress-induced damage accumulation.[30] This approach has several advantages. First, field and experimental studies display inelastic deformation of complex networks of fractures that cannot be explained by elastic analysis. Second, damage mechanics does not require any special assumption, such as initial perturbations or non-realistic high stresses. Third, damage fracturing does not suffer from the present computational limitations of local element enrichment formulations (e.g., the extended finite element method (XFEM)).[31]

2.2. Continuum damage mechanics (CDM)

With this study we aim to model the typical failure mechanisms occurring around boreholewalls shortly after drilling, as observed in laboratory experiments. It was

observed that the mechanism of breakout development is governed by tensile spalling and shear fracturing.16, 17 An attempt was made to model those failure mechanisms by taking into account the different strength criteria for tension and compression in the modeling procedure. Because the responses of a quasi-brittle material to tensile and compressive failure are quite different, it is not sufficient to represent the failure processes by a single parameter. Hence, following,[8]the parameters of the plasticity used herein are decomposed into a tension and a compression part.

2.2.1. Framework of plastic-damage model

The theory of continuum damage models has been developed using a thermodynamical approach.[3] The constitutive equations for this plastic model and its thermodynamicinterpretation can be found in Lemaitre.[32] In this model, the concepts of elastic modulus (E) and stiffness reduction with increasing microcrack density are applied by using a damage parameter D as a dimensionless approximation for stiffness degradation. In the initial stage, D=0 (no degradation) and, at failure, D=1, the material is completely damaged and the stress drops to zero.

(1)EE0=(1−D)

where E and E0 are the current and initial elastic moduli of the material, respectively. Decomposing strain into elastic (εe) and plastic strain (εp)and incorporating the damage parameters, the stress-strain relationship can be written as follows

(2)σeff=(1−D)(E0)(ε−εp)

where σeff is the effective stress. The effective stress concept (here unrelated to the pore pressure) is used to degrade the elastic stiffness, which in turn controls the flow rule and the shape of the yield surface.

The plastic strain represents all irreversible deformations including those caused by microcracks. An internal variable of damage state κ is used to represent the impact of those deformations to the elastic properties of the material. The development of damage parameter D in Eqs. (1), (2) is then determined as a function of the damage state, D=f(κ).

Following Lubliner et al. [4] the damage variable, denoted by 0≤κא≤1, is defined by

(3)κא=1gא∫0εpσא(εp)dεp

(4)gא=∫0∞σא(εp)dεp

To distinguish tensile and compressive damage, the variable א∈{t,c} is used. It is uniaxial tensile for א=t and uniaxial compressive for א=c. The term gא is the normalized energy during microcracking. For a continuum framework gא is the energy released during compressive or tensile fracturing Gא normalized by a localization

size, lא[8] (gא=Gאlא). The value of lא is a characteristic length associated with an integration point.

Since the relation between plastic strain and damage parameter strongly depends on the rock properties, laboratory measurements are mandatory to define the connection between both parameters. Abundant laboratory tests are available in the literature, yet only very few numerical studies have been performed to determine the damage law of a rock based on laboratory data. Busetti[18] created a numerical model based on the triaxial laboratory measurements on Berea sandstone. A damage law describing the hardening and damage evolution of the material resulted (Fig. 1). We will use their results and apply it to the wellbore problem.

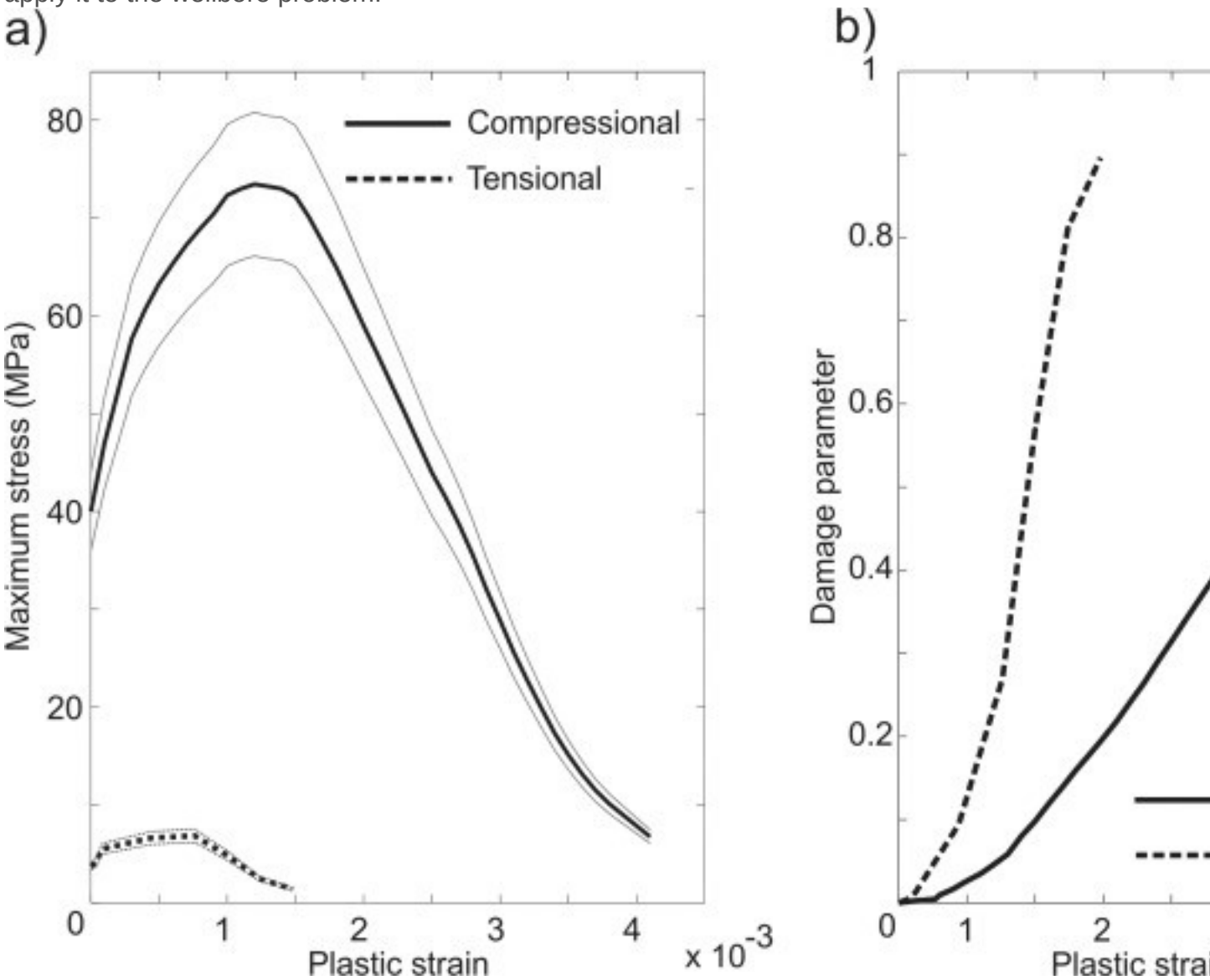

1. Download high-res image (324KB)

2. Download full-size image

Fig. 1. Damage law of strain (a) and damage (b) evolution obtained by Busetti et al.[18] for Berea Sandstone. The rock is about 10 times stronger in compression. The gray lines in (a) indicate the 10% variation of the rock strength applied in the parameter study.

The yield surface evolves with the damage variable and limits the current admissible stress. Taking into account *both the tensile and compressional failure mechanism*, the admissible stress states are constrained such as

(5)F(σeff,κ)≤0

With this framework, the elastoplastic responses are described only in terms of σeff and κ. The equations of the yield surface and the flow rule as well as the numerical technique used in this study to handle the numerical problem that might occur during softening phase of plastic deformation are described in Appendix A. The present constitutive system can be implemented effectively for numerical computation, because the solution for the elastoplastic response is separate from the degradation damage process.

2.2.2. Fracture energy

In this study, CDM is used to describe the local evolution of microcracks in the vicinity of wellbore, instead of explicitly model the fracture propagation. This can be done because the CDM concept and fracture mechanics are thermodynamically equal according to the equivalent crack concept ,[33] which states that there exists a damage zone that is equivalent to a discrete fracture and vice versa. In the present formulation, this manifests in the normalized dissipated energy term g. The energy consumed by forming all of the microcracks in a volume is equivalent to decohesion of singular cracks with surface area Ad:

(6)∫V−YDdV=GAd

where Y is the damage energy release rate. Following Mazars,[34] an equivalent crack, Ae is attained from Eq. (7).

(7)Ae=∫V∫0D(x)−YDddxGf

where ddx represents evolution of the damage at a point, x. The total damaged area then reflects the summation of the area comprising all equivalent cracks over a volume, V. This equivalence also offers a mean for comparison between numerically predicted damage and the damage observed in experiments and quantified using other stiffness reduction models.

3. Numerical modeling of CDM

The CDM presented has been implemented in a standard finite element program for non-linear analysis. The commercial finite element software Abaqus (Simulia) is used in this simulation. We intend to model the stress concentration around a borehole and the damaging process that follows. Plastic strain is assumed to be caused by the accumulation of microcracks during the damaging process and is decomposed into compressive and tensile part to highlight the different failure mechanisms involved.

3.1. Numerical procedure and borehole model

In order to compute the stresses around a vertical wellbore, we model a 2-D slice orthogonal to the wellbore axis. The model is meshed with four-node linear quad elements with mesh density increasing in the vicinity of borehole (Fig. 2). A plane strain assumption is applied in the modeling scheme. Taking advantage of the symmetric stress distribution in an isotropic medium, only a quarter of the wellbore is modeled to reduce the computational time.

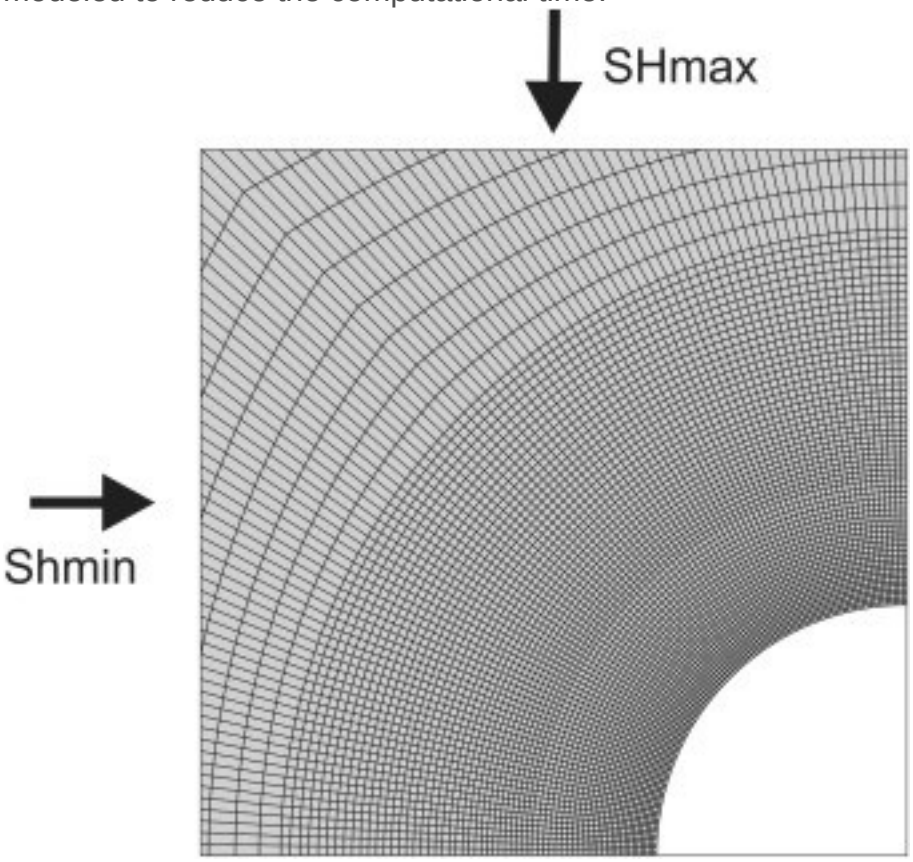

1. Download high-res image (730KB)
2. Download full-size image

Fig. 2. A close up of the refined mesh around the wellbore. S_{Hmax} and S_{hmin} are plotted in vertical and horizontal directions, respectively.

To incorporate the CDM approach, we use the concrete damage plasticity capability of the finite element suite Abaqus/Explicit.[35] It is well suited for extreme nonlinearity such as strain localization. We found that implicit solutions had difficulty converging during strain softeningand terminated shortly after failure. Although the constitutive relationship is time independent (i.e., inferring quasistatic deformation), the Abaqus/Explicit solver integrates through time by using many small time increments to find the steady state solution.
The algorithm of the borehole breakout modeling can be explained as follows. We apply the initial stress at the mesh to model the stressed rock in the underground. Displacement boundary conditions are chosen, i.e. the outer nodes are fixed and the inner nodes of the wellbore wall are free. At the beginning of the simulation the nodes at the wellbore wall are fixed to simulate the undisturbed rock. Drilling of the well is simulated by instantaneous release of this boundary condition. The elastic and plastic deformation at each node and time steps are calculated using the equations presented in the Appendix A. The damage law is then used to determine the damage state at each node based on the evolution of the elastoplastic step. The effective stress and the stiffness of the material is then updated based on the damage level at each step. Hence, it represents a transient process of damage propagation in a stressed material. The simulation ends after a steady state is reached, i.e. no more plastic deformation accumulates.
It is possible to take into account the effect of the weight of the mud, which usually is used to stabilize the wellbore, by applying a radial pressure to the borehole wall. While in principal any orientation of the wellbore can be modeled by our model set up, results shown hereafter are for the case of a vertical wellbore.

The Busetti[18] damage law is taken as basis for the CDM model. The damage parameter, for both tensile and compressive damage, is limited to 90%. This was made to prevent extreme plastic strains at highly damaged elements. Despite this limitation it can be seen in the following results that highly damaged elements show strong plastic deformation. In terms of borehole breakout development, it can be assumed that those elements would be easily washed off by the circulation of the drilling mud during the drilling process and leave a breakout at the wellbore wall.
In a pre-stressed medium, the instantaneous release of the boundary condition at the borehole wall will create rapid deformation around the borehole. Rayleigh damping is used in order to reduce the deformation rate and allow convergence of the solution of the deformation problem. This damping makes the system viscous by creating an

additional damping stress proportional to the total strain rate. To prevent numerical artefacts that might occur by introducing damping into the modeling scheme, only a small value of stiffness-proportional Rayleigh damping (0.0015) is used. Another parameter that affects the simulation time is mass scaling.[36] A reduction of the density by a factor of 2 is used in order to reduce the computational time. In this case, although the results showed herein represent the transient process of damage propagation, our time scale does not correspond to the real time scale these processes occur on .[37] Therefore, in this paper, the transient process of the damage propagation in the vicinity of borehole is shown in the normalized time.

3.2. CDM synthetic borehole breakout modeling

The parameters used in this simulation are listed in Table 1. For testing purposes, the model was first run using an elastic medium and compared to the analytical Kirsch solution.[38] A perfect match was obtained between the numerical and the analytical solutions. The code is then run for a synthetic plastic medium with a modified damage law from Busetti et al.[18] A borehole with radius equal to 10 cm is modeled. This model is pre-stressed with a far fieldeffective stress with a magnitude of 25 MPa and 60 MPa for the minimum (S_{hmin}) and the maximum horizontal stress (S_{Hmax}), respectively, and 40 MPa for the vertical stress (S_v). This model is built to represent the production borehole in the typical oil and gas reservoir at a depth of around 2.5 km. No mud pressure in excess of the formation pressure stabilizing the well is incorporated in this synthetic test run.

Table 1. Model parameters for the breakout simulation in Berea sandstone.

Density (ρ)	2100 kg/m^3
Young's modulus (E)	23.2 GPa
Poisson's ratio (υ)	0.17
Dilation angle (θ)	15°
Eccentricity (*e*)	0.1
Ratio of initial equibiaxial compressive yield stress to initial uniaxial compressive yield stress (σb0σc0)	1.16
Stress intensity factor (Kc)	0.66
Effective maximum horizontal stress (S_{Hmax})	60 MPa
Effective minimum horizontal stress (S_{hmin})	25 MPa
Effective vertical stress (S_v)	40 MPa

Fig. 3 shows the stress and damage evolution as a function of strain in the element at the borehole wall in the direction of the S_{hmin}. This element is subjected to the highest compressive stress concentration and is the first element to be damaged. At the early

step the element is still in the elastic mode. A linear increase of stress with increasing strain is observed. At strain ε=0.0015, the stress concentration is larger than the yield strength and plastic deformation starts to accumulate. The element is entering the hardening phase of the plastic deformation. At this stage, stress increases with increasing strain but at a lower rate than during the elastic loading. Fig. 4.a shows the stress, strain and damage in the mesh at the end of the hardening phase. S_{hmin} is plotted in the horizontal direction and, since we focus only on the borehole breakout development, only the region within 30° from S_{hmin} is plotted in the numerical results showed herein. Only plastic strain is shown in this figure as the purpose is to analyze the development of the plastic deformation in the model. It can be seen that the plastic deformations take place only in the vicinity of the borehole wall and very low plastic strain is present at this stage. The damage value is also very low, which means that the elastic properties of the element is not altered by much, hence the stress concentration is very similar to the one obtained for the elastic medium.

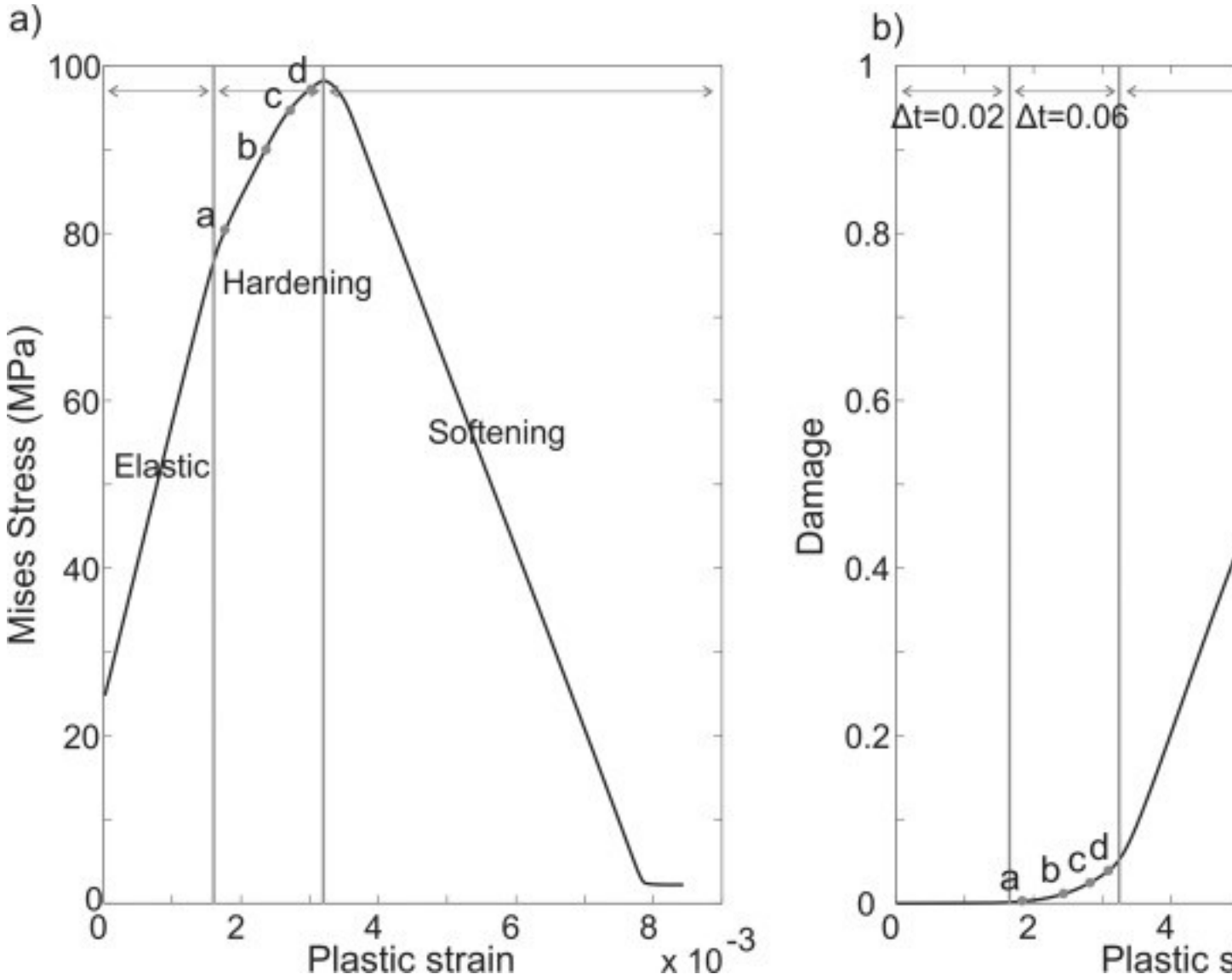

1. Download high-res image (287KB)
2. Download full-size image

Fig. 3. Graphic of the stress (a) and damage (b) as a function of total strain measured at the first damaged element of the model. The element is located at the borehole wall along the direction of S_{hmin}. The stress and damage state at the node for the different applied S_{Hmax} are also plotted in gray dots, i.e. a=45 MPa, b=47 MPa, c=49 MPa, d=51=MPa.

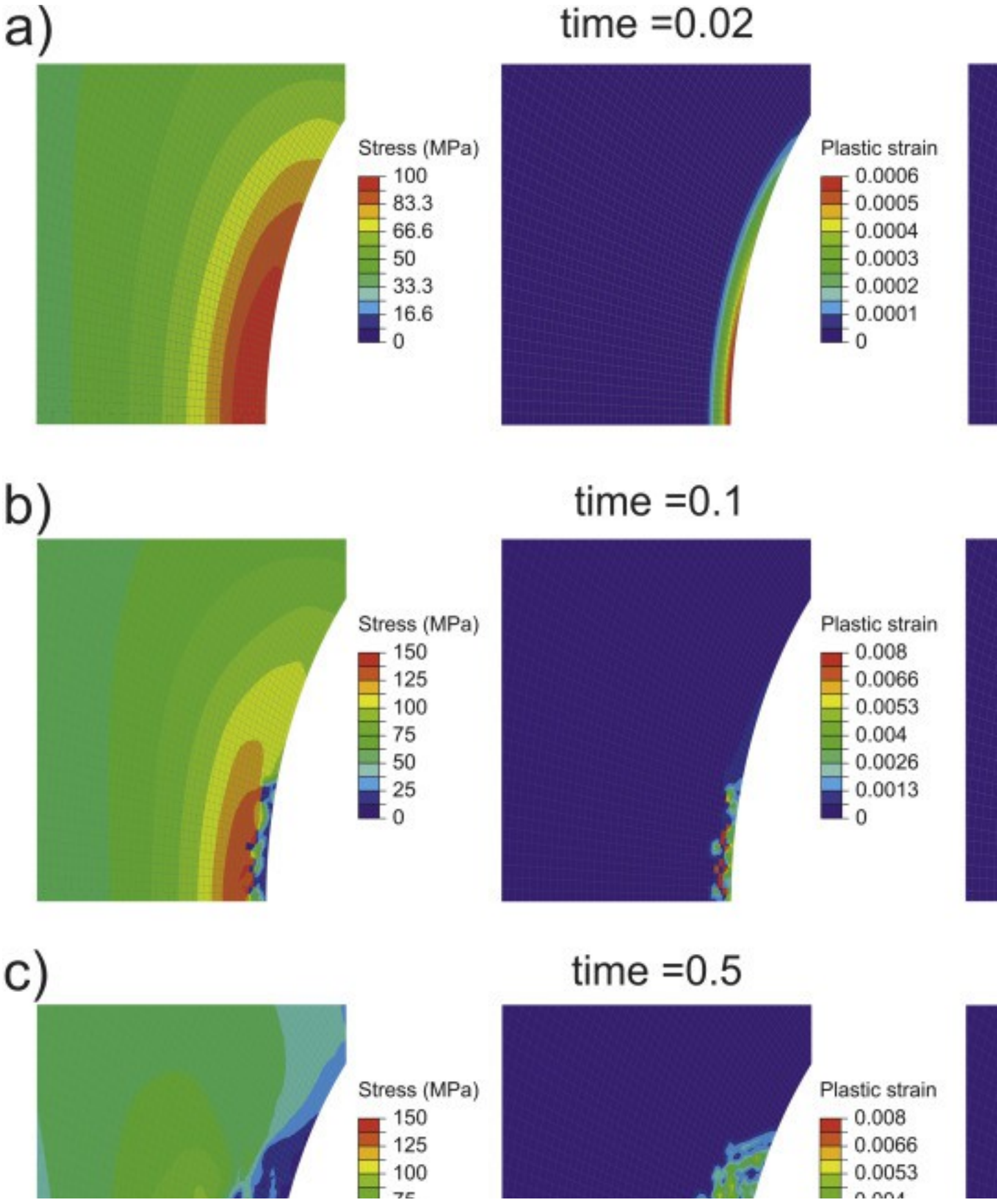
a)
time =0.02
Stress (MPa)
100
83.3
66.6
50
33.3
16.6
0
Plastic strain
0.0006
0.0005
0.0004
0.0003
0.0002
0.0001
0
b)
time =0.1
Stress (MPa)
150
125
100
75
50
25
0
Plastic strain
0.008
0.0066
0.0053
0.004
0.0026
0.0013
0
c)
time =0.5
Stress (MPa)
150
125
100
Plastic strain
0.008
0.0066
0.0053

1. Download high-res image (3MB)
2. Download full-size image

Fig. 4. The evolution of von Mises stress (left), plastic strain (middle) and damage (right) around borehole during simulation. The simulation end after a steady state is reached. The simulation time is normalized by the time required to reach the steady state solution.

With increasing time the element then eventually enters the softening phase. This phase occurs very fast and increases the value of both damage and plastic strain significantly to the final damage state. It can be seen in Fig. 3.a that the stress at the damaged element decreases to 3 MPa (very small compared to the 98 MPa at the end of the hardening phase). Interestingly, a high stress concentration is observed at the tip of the damage area. This high stress concentration drives the damage area further inside the rock mass. Fig. 4shows the development of the damage area with time. It can be seen that the damage area propagation is governed by the high stress distribution at the damage front. At the end of the simulation, time t=1, the second invariant of the stress deviator at the damage front is very high. However, the first stress invariant is also high. The first stress invariant acts as the normal stress in the Mohr-Coulomb criterion. The increase of the magnitude of this stress invariant makes the stress concentration at the damage front fall below the yield surface. Hence, the model has reached the stable condition. At the end of the simulation, a wide and deep damaged area is formed (Fig. 4.d). In sandstone, under high values of compressive stress, tensile splitting is suppressed and only shear failure, i.e. compressional damage, occurs in this simulation. Fig. 5 shows the number of damaged elements and the evolution of plastic strain as a function of time. The analysis is done at elements within 1.2 times the borehole radius and within 30° from S_{hmin}. This is the area where most of the plastic deformation took place. It can be seen that both the mean plastic strain and the number of damaged elements increases significantly following the damage of the first element (time t=0.08). After time t=0.6 the slope of both graphs decreases and it approaches the stable condition at time t=0.95. After this time, no more plastic deformation occurs. The flat line in both graphs starting at time t=0.95 till the end of the simulation indicates that the simulation has reached a stable equilibrium condition. The time required for the simulation to reach the stable condition depends on the far field stress. High differential stress creates a larger damaged region and requires a longer simulation time.

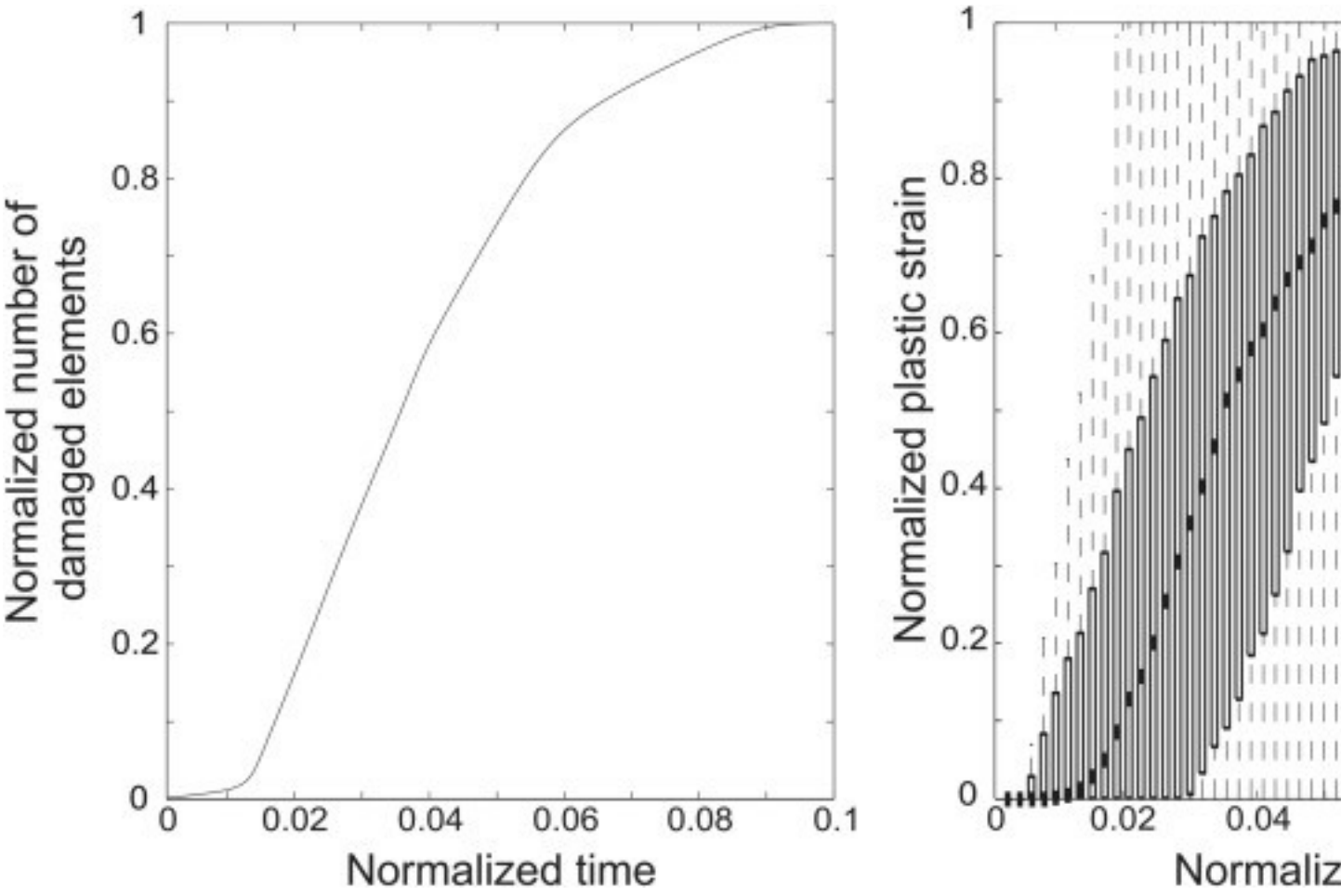

1. Download high-res image (369KB)
2. Download full-size image

Fig. 5. (a) The evolution of the number of damaged elements and (b) the distribution of plastic strain in all elements as a function of time drawn as boxplots. The values of all parameters, i.e. damaged elements, plastic strain and time, are normalized.

3.3. Sensitivity test

In simulations involving softening processes mesh dependency needs to be accounted for. Several models with element sizes at the wellbore wall ranging from 1.5 mm to 3 mm are used to check the consistency of the results. The outer shape of the damage area is picked as a proxy for the outer boundary of the breakout. The variation of the breakout size is entirely within the element size used. Hence it can be concluded that the geometry of the damage area obtained in our simulation is consistent for different element sizes. Although the element size does not influence the inferred size and shape of breakouts, the internal structure of highly damaged zone obtained in this numerical simulation (Fig. 4.d) is mesh-dependent, i.e. the finer element size the more structures

are observed. In addition, Rayleigh damping also affects the affect the thickness of the high damage/plastic-strain structures shown in Fig. 4.d, i.e. the bigger the damping, the thicker the structures are. Hence, we do not interpret this internal structure. A more sophisticated constitutive scheme is required in order to model those local failure processes, e.g. Cosserat continuum .[39]

When we compare our simulation with laboratory experiments, one source of discrepancy is the uncertainty in the mechanical rock parameters reported for laboratory experiments, e.g. Young's modulus, Poisson's ratio and the compressional and tensile strength of the material. The influence of each parameter is investigated by a set of simulations where we vary material properties within 10% of their default values listed in Table 1. Table 2 lists the resulting variation of breakout depth and width for each parameter tested. The geometry variation is represented in percentiles relative to the geometry obtained with the default parameters. It can be seen that the Poisson's ratio affects breakout size stronger than Young's modulus both concerning depth and width of the breakout. The strength of the rock affects breakout size the most, as it governs the failure processes in the simulation. In general, it can be concluded that varying the mechanical properties by 10% will vary the breakout size by 12% and 17% for width and depth, respectively.

Table 2. The variation of the geometry, width and depth, of the damaged area in percent relative to the one obtained with parameter listed in Table 1 for 10% material properties uncertainty.

Rock property	Breakout width	Breakout depth
Young's modulus	7%	10%
Poisson's ratio	10%	13%
Rock strength (Compressive and tensile)	12%	17%

4. Analysis of borehole breakout

An understanding of the breakout phenomenon is important for determining in-situ stress. The relation between the magnitude of the far field stress and size of breakouts is of particular importance for stress measurement using borehole breakouts. Previous studies of borehole breakouts indicated that failure of the borehole wall in a sedimentary rock is often governed by shear fracturing, along one or more shear fractures extending from the borehole wall into the rock.[16], [40] The shear fractures can cause breakouts as they intersect .[41] This creates a breakout with a wider area at the borehole wall and a pointy end in the formation. We intend to use the results of the CDM modeling in order to explain the failure processes involve in the breakout development that are typically observed in sedimentary rock.

Based on the numerical modeling results, the very first stage of breakout development is the development of the small plastic strain area very close to the borehole wall in S_{hmin} direction. This is similar with the initiation of small intergranular cracks at the highest stress-strength ratio area at a low applied stress observed in the laboratory experiments e.g. Haimson,[21]Ewy and Cook.[19] The damage area cannot penetrate deeper because the overstressed area in the vicinity of the borehole wall does not extend very deep into the rock and the stress level remains below the rock strength.
A set of simulations with applied S_{Hmax} varying from 45 MPa to 55 MPa is performed in order to understand this low damage stage better. It is found that with increasing applied S_{Hmax} the plastic strain is also growing but does not enter the softening phase if the magnitude of S_{Hmax} remains less than 52 MPa (Fig. 3). After this critical stress the elements enter the softening strain phase, and the damage propagates further. This softening phase might represent the initiation of fracturing through the matrix that is observed in experiments at high applied stress. The fracture toughness of the matrix is typically weaker, thus cracks will continue to extend following the path of least resistance that takes them into the formation.
It is interesting to note that the breakout grows wider and deeper at the beginning but after time t=0.4 the damage area only grows deeper. It is in agreement with the hypothesis from the early work of Zoback et al.[40] and Zheng et al.[9] which showed that the redistribution of stress around a broken out borehole deepens the failed zone but does not widen it. The microscopic observation of borehole breakouts in sandstone by Ewy et al.[19] also revealed the growth of splitting cracks oriented tangential to the borehole wall, starting with a long splitting crack very close to the borehole wall and deepening with a short crack towards the rock formation. Haimson[21] showed (figure 19 in his paper) the spallation zone which develops wider initially before it is deepening during the later stages of breakout formation. We conclude that, at least for sandstone, the CDM model is able to reproduce similar failure features as observed in laboratory experiments.

4.1. The effect of far field stress

The results presented in the previous chapter need to be compared with data from field measurements and laboratory tests to assess the reliability of the numerical model developed in this study with the aim to predict the breakout geometry. A direct comparison in the same rock material could not be made. However, Haimson and Lee[20] performed a series of laboratory drilling simulations in Tablerock sandstone samples under varying stress conditions. Both Tablerock and Berea sandstones are

arkosic sandstones which have similar characteristics such as porosity around 15%, they contain 50–80% of sub-angular quartzgrains, complemented primarily by feldspar, and some clay. They are well cemented with micro-crystalline quartz and clay minerals. Although the mechanical properties of the two sandstones are slightly different (Table 3), the failure mechanisms that lead to breakout development are similar, i.e. fracturing through the matrix and the development of the episodic spallation zone, while the final shape of both breakouts is also comparable.[21]Therefore, the Busetti damage law[18] can still be used for breakout simulation in Tablerock sandstone. A lower value of 18.5 GPa and a higher value of 0.23 were used for Young's modulus and Poisson's ratio, respectively, to represent the elastic properties of Tablerock sandstone (Table 3). A set of simulations with the same applied stress levels as the one applied in Haimson and Lee[20] is performed. This test can be used to find a correlation between the applied stress and the breakout geometry.

Table 3. Mechanical properties of Tablerock sandstone[20] and Berea sandstone.[42]

Rock property	Tablerock sandstone	Berea sandstone
Elastic modulus	18.3±0.14 GPa	25.25±2.14 GPa
Poisson's ratio	0.23±0.07	0.25±0.08
Uniaxial compressive strength	39.5 ± 4.8 MPa	49 ± 8.2 MPa
Tensile strength	4.4 ± 0.2 MPa	6.8 ± 3 MPa

We defined breakout as the area within the outermost structure of the totally damaged elements, i.e. D=0.9. Based on this definition, the width is estimated from the angular distance of the two elements at the other end of the damaged area at the borehole wall and the depth is the distance from the borehole wall to the deepest damaged element. The width and the depth of the breakout for each simulation are plotted in Fig. 6, together with the results from Haimson and Lee.[20] The depth of the breakout is normalized by the radius of the borehole. For most stress conditions the breakout dimensions and specifically its trend with increasing S_{Hmax}/S_{hmin} ratio is reproduced very well by our CDM model. A significant deviation of the breakout width is observed for the S_{hmin} =40 MPa, S_v =50 MPa set, with a lot wider observed breakouts in the laboratory experiment. The trend with increasing S_{Hmax}/S_{hmin} ratio is captured however. For this stress setting the variation of the hoop stress along the borehole wall is relatively weak and hence the breakout zone is weakly localized. The breakout depth however, is matched very well by the simulation. The deviation of breakout depth for the S_{Hmax} =70 MPa, S_{hmin} =25 MPa and S_v =40 MPa set appears to be caused by an outlier in the laboratory experiments. This demonstrates that there is a considerable uncertainty due to the

microdefect of the sample at a granular scale that might affect the experiment results. For the S_{hmin}=20 MPa, S_v=40 MPa set we do not achieve a satisfactory fit of the trend of breakout depth with increasing S_{Hmax}/S_{hmin} ratio. We could only speculate about the reasons but clarification would require a more extensive testing program on Tablerock or Berea sandstones. All other breakout dimensions obtained from our simulations fall within 15% of the corresponding experimental one.

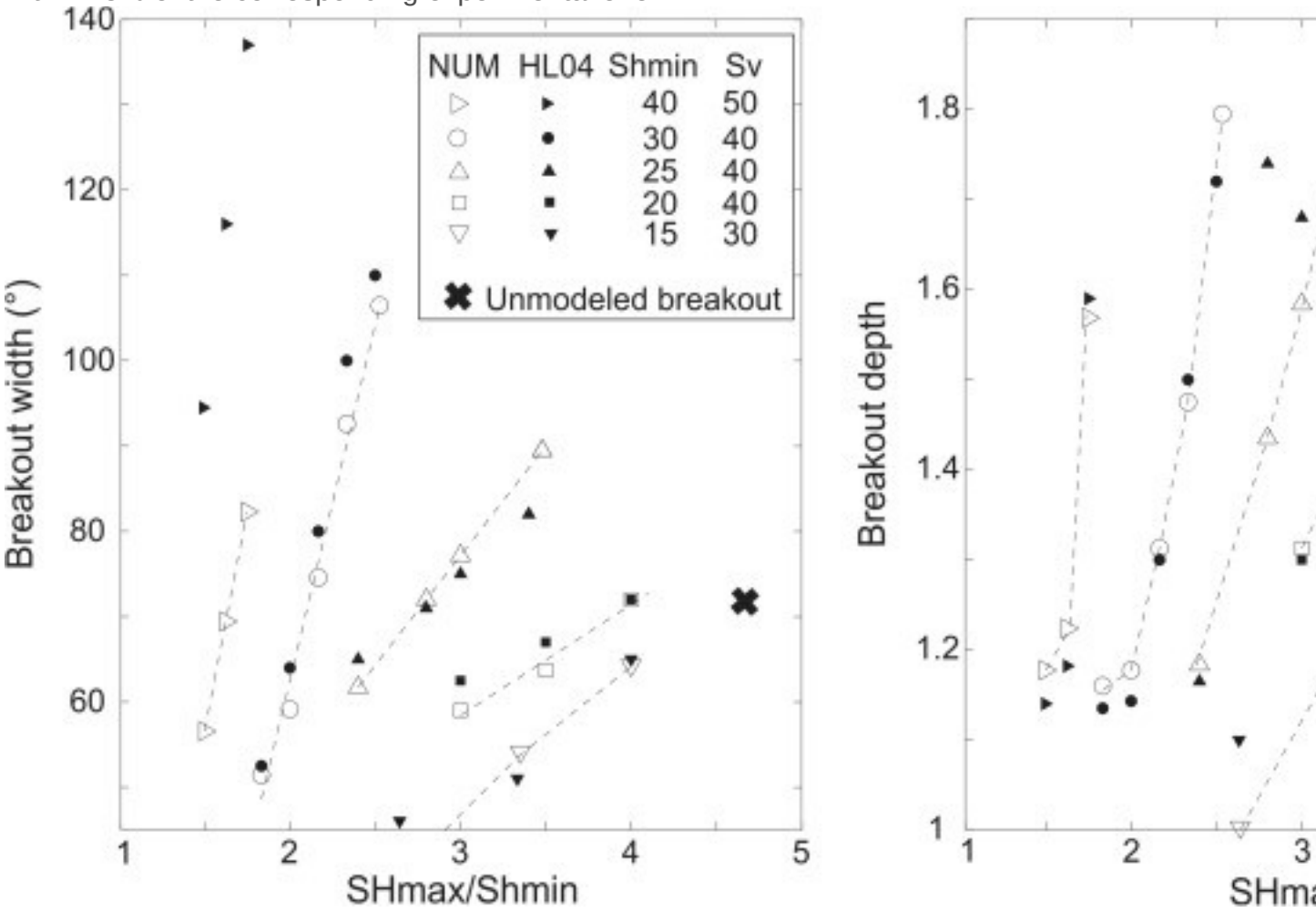

1. Download high-res image (270KB)
2. Download full-size image

Fig. 6. Variation of the breakout width (a) and the breakout depth normalized with the borehole radius (b) as a function of the far-field horizontal principal stress ratio S_{Hmax}/S_{hmin}. Blank and filled marks are for numerical (NUM) and laboratory (HL04) results , [20] respectively.

For the set S_{Hmax} =40 MPa, S_{hmin} =15 MPa and S_v =30 MPa, the borehole wall stays in the hardening phase, hence only small deformation is observed in the vicinity of the borehole wall. This is expected since Berea sandstone has a higher compressional

strength compared to Tablerock sandstone (Table 3). Thus a higher differential stress is required to cause damage in the material. One experiment with a rather extreme horizontal stress ratio of 4.67 could not be simulated (marked with black cross sign). In this extremely high stress ratio the well is squeezed, a rapid deformation towards the S_{hmin} direction will occur at a very high strain rate and the numerical calculation did not converge.

In general, it can be seen that the numerical and experimental results match quite well. The differences between the numerical and experimental results can be partially explained by the inherent variation of material properties. The CDM concept implemented in this simulation allows us to reproduce breakout geometries obtained through laboratory experiments. Simulation allows furthermore to perform variation of the conditions that could not be achieved in the laboratory experiments, e.g. high temperature and pressure condition, at a greater scale comparable to the reservoir. The relation between the geometry of breakout with increasing applied S_{Hmax} at fixed $S_{hmin}$and S_v is expressed by the dashed lines in Fig. 6. It can be seen that the breakout depth shows a non linear increase with stress ratio. This is obvious when S_{hmin} is held at 30 and 40 MPa, and S_v at 40 and 50 MPa, respectively (right-pointing triangle and circle symbols in Fig. 6.b). In this setting, we see that at a lower S_{Hmax}/S_{hmin} ratio a small gradient of breakout depth increase with stress ratio is observed, but the gradient is much stronger towards a higher horizontal stress ratio. While at the lower S_{hmin} and S_v setting, only the trend of strong increase of breakout depth with stress ratio is captured, which might be due to the S_{Hmax}/S_{hmin} ratio being high. A closer to linear trend is observed between the breakout width and the horizontal stress ratio. However, the gradient of the trend tends to decrease from left to the right, indicating that the width changes are bigger in the higher stress regime. There is a correlation between the depth and the width of breakouts, with both growing with the applied S_{Hmax} with the constant S_v and S_{hmin}. The implication here is that the two breakout characteristics are not independent of each other and therefore only one far field principal stress can be estimated from breakout geometry information, if the other two principal stresses were known in advance.

5. Discussion and conclusion

The CDM concept can model the onset, evolution and stabilization of failure in boreholebreakout. This approach takes into account the changes of the elastic material as a result of the damaging process. Previous experimental studies on damage mechanics have shown that increasing crack damage within rock alters the elastic

moduli in rocks significantly (Katz and Reches,[29] Faulkner et al.).[43] Heap et al.[26] have conducted experimental measurements of changes in elastic moduli with increasing applied stress on a range of different rock types. They show that the trend in elastic moduli evolution with increasing damage was different for each rock type with Young's modulus decreasing by 11–32% and Poisson's ratio increasing by up to 600%. The simulation results obtained in this study have shown that already a 10% variation in the elastic properties can significantly affect the geometry of the damaged area. Given the variation of the two elastic parameters obtained in the laboratory, it can be concluded that the geometry of the damaged area formed will vary strongly for different rock types. Changes of the damage law do not only affect the geometry of the damaged area, but also the failure mechanism involved in the breakout development. In this study, the damage process is dominated by compression, hence only shear fracturing is observed. Busetti et al.[44] showed that for Berea sandstone reservoirs, tensile damage starts to develop after the material suffered high plastic damage. In our borehole breakout modeling, the high compressive stress in the vicinity of the borehole prevents the material from having such a high plastic deformation, hence only compressive damage is observed. Failure mechanisms might be different for other rocks. For instance, in crystalline rock a limited degree of plastic deformation occurs on a much shorter time-scale before brittle failure starts than in Berea sandstone.[45]

Using CDM we are able to match the key characteristics of the failure process during the breakout development as observed in experimental tests. The development of the damage area is shown to be governed by the stress concentration at the damage front until it dissipates and finally reaches a stable condition. Even with limited experimental data and constitutive damage laws available, CDM could be successfully applied yielding a good agreement between experimental laboratory and simulation data. We successfully transferred the constitutive relations derived for Berea sandstone and applied it to Tablerock sandstone. This demonstrates the wide applicability of the CDM approach to these kinds of problems.

It has been shown that width and depth of borehole breakouts are not independent of each other and the relation between the geometry of breakouts and the magnitude of the principal stress is non-linear. Our simulations support the hypothesis of Haimson and Lee[20] that only one far-field principal stress components, i.e. S_{Hmax} in a vertical well, can be estimated from breakout geometry. This requires, however, that the other two principal stresses are known and sufficient appraisal of the constitutive damage laws exist.

Our effort presented here is in line with the recent focus on plastic deformation in tunneling and drilling. Describing failure is critically dependent on the constitutive damage law. Hence, additional laboratory testing to determine constitutive damage laws as well as the strength and yield criteria need to be conducted in order to better understand breakout formation in various types of rock. This modeling scheme could be developed further by accounting for a poroelastic medium to better represent the in-situ rock condition. A more sophisticated numerical scheme needs to be used to be able to model the localized damage pattern which might represent the spallation processes at the borehole wall. Nevertheless, it was shown that by using elements with aspect ratios close to one, we can explain the complex fracturing process that leads to breakout formation through the continuum damage mechanics concept.

Acknowledgements

The authors acknowledge the funding to D.S. from the Indonesia Directorate General of Higher Education (DIKTI), the German Academic Exchange Service (DAAD). M.S. was supported by the Alexander von Humboldt Foundation and the Stanford Center for Induced and Triggered Seismicity. Additional support from the Energie Baden-Wuerttemberg (EnBW) and the Helmholtz Association of German Research Centres is appreciated. D.S. also thanks Klaus Regenauer-Lieb that helped through his insight.

Appendix A

The CDM approach used herein makes use of the yield function proposed by Lee and Fenves[8] to account for the different evolutions of strength under tension and compression. In term of stress invariants, the yield function takes the form

(A.1)$F=11-\alpha(3J2+\alpha I1+\beta\sigma max-\gamma\sigma max)-\sigma c(\varepsilon cp)=0$

with

(A.1.a)$\alpha=\sigma b0\sigma c0-12(\sigma b0\sigma c0)-1;0\leq\alpha\leq0.5$

(A.1.b)$\beta=\sigma c(\varepsilon cp)\sigma t(\varepsilon tp)(1-\alpha)-(1+\alpha)$

(A.1.c)$\gamma=3(1-Kc)2Kc-1$

where $I1=tr(\sigma)$ is the first stress invariant, $J_2=12tr(s2)$ is the second invariant of the deviatoric stress tensor s, σmax is the maximum principal stress; $\sigma b0\sigma c0$ is the ratio of initial equibiaxial compressive yield stress to initial uniaxial compressive yield stress; Kc is the stress intensity factor; $\sigma t(\varepsilon tp)$is the tensile cohesion stress; and $\sigma c(\varepsilon cp)$ is the compressive cohesion stress.

A flow rule, which is assumed to be a non-associated potential plastic flow rule, is then used to evaluate the plastic strain. The flow rule can be written as:

(A. 2)G=(eσt0tanθ)2+J2−2−I1tanθ…….

where θ is the dilation angle measured in the $I_1 - J_2$ plane at high confining pressure, σt0 is the uniaxial tensile stress at failure; and *e* is the eccentricity. For further details on the theoretical description we refer the reader to Lee and Fenves[8] and Lubliner et al.[4]

The combination of strain softening and damage permits simulation of extreme localized weakening, where material degrades to zero strength, which might lead to a numerical instability. The CDM developed in this study uses the concept of Hillerborg's[46] fracture energy-based damage and stiffness degradation in continuum damage mechanics is used. With this approach the rock's brittle behavior is defined by a stress-displacement response rather than a stress-strain response. This concept is implemented by defining a characteristic length associated with an integration point. By using square elements, we reduce possible numerical errors that can occur during modeling of the softening phase of plastic deformation.

References

1

L.M. Kachanov**Time of the rupture process under creep conditions**

Izv Akad Nauk {S.S.R.} Otd Tech Nauk, 8 (1958), pp. 26-31

View Record in Scopus

2

Y.N. Rabotnov**Kinetics of creep and creep rupture**

H. Parkus, L.I. Sedov (Eds.), Irreversible Aspects of Continuum Mechanics and Transfer of Physical Characteristics in Moving Fluids, Springer, Vienna (1968), pp. 326-334

CrossRefView Record in Scopus

3

J. Chaboche**Continuous damage mechanics—a tool to describe phenomena before crack initiation**

Nucl Eng Des, 64 (2) (1981), pp. 233-247

ArticleDownload PDFView Record in Scopus

4

J. Lubliner, J. Oliver, S. Oller, E. Oñate**A plastic-damage model for concrete**

Int J Solids Struct, 25 (3) (1989), pp. 299-326

ArticleDownload PDFView Record in Scopus

5

C.C. Roth, D. Mohr**Effect of strain rate on ductile fracture initiation in advanced high strength steel sheets: experiments and modeling**

Int J Plast, 56 (0) (2014), pp. 19-44
ArticleDownload PDFView Record in Scopus

6

J. Mazars, F. Hamon, S. Grange**A new 3D damage model for concrete under monotonic, cyclic and dynamic loadings**
Mater Struct (2014), pp. 1-15

7

V.S. Deshpande, A.G. Evans**Inelastic deformation and energy dissipation in ceramics: a mechanism-based constitutive model**
J Mech Phys Solids, 56 (10) (2008), pp. 3077-3100
ArticleDownload PDFView Record in Scopus

8

J. Lee, G.L. Fenves**Plastic-damage model for cyclic loading of concrete structures**
J Eng Mech, 124 (8) (1998), pp. 892-900
CrossRefView Record in Scopus

9

Z. Zheng, K. Kemeny, N. Cook**Analysis of borehole breakouts**
J Geophys Res, 94 (B6) (1989), pp. 7171-7182
CrossRef

10

D. Sahara, M. Schoeball, T. Kohl, B. Mueller**Impact of fracture networks on borehole breakout heterogeneities in crystalline rock**
Int J Rock Mech Min Sci (2014)

11

J.B. Cheatham Jr**A new hypothesis to explain stability of borehole breakouts**
Int J Rock Mech Min Sci Geomech Abstr, 30 (7) (1993), pp. 1095-1101
ArticleDownload PDFView Record in Scopus

12

P.A. Nawrocki, M.B. Dusseault**Modelling of damaged zones around openings using radius-dependent Young's modulus**
Rock Mech Rock Engng, 28 (4) (1995), pp. 227-239
CrossRefView Record in Scopus

13

E. Detournay, C. Fairhurst**Two-dimensional elastoplastic analysis of a long, cylindrical cavity under non-hydrostatic loading**
Int J Rock Mech Min Sci Geomech Abstr, 24 (4) (1987), pp. 197-211
ArticleDownload PDFView Record in Scopus

O. Gaede, A. Karrech, K. Regenauer-Lieb**Anisotropic damage mechanics as a novel approach to improve pre- and post-failure borehole stability analysis**
Geophys J Int, 193 (2013), pp. 1095-1109
CrossRefView Record in Scopus

15

M. Schoenball, D.P. Sahara, T. Kohl**Time-dependent brittle creep as a mechanism for time-delayed wellbore failure**
Int J Rock Mech Min Sci, 70 (2014), pp. 400-406
ArticleDownload PDFView Record in Scopus

16

I. Vardoulakis, J. Sulem, A. Guenot**Borehole instabilities as bifurcation phenomena**
Int J Rock Mech Min Sci Geomech Abstr, 25 (3) (1988), pp. 159-170
ArticleDownload PDFView Record in Scopus

17

A. Guenot**Borehole breakouts and stress fields**
Int J Rock Mech Min Sci, 26 (1989), pp. 185-195
ArticleDownload PDFView Record in Scopus

18

S. Busetti, K. Mish, Z. Reches**Damage and plastic deformation of reservoir rock: Part 1. Damage fracturing**
AAPG Bull, 96 (9) (2012), pp. 1687-1709
CrossRefView Record in Scopus

19

R.T. Ewy, N.G.W. Cook**Deformation and fracture around cylindrical openings in rock—II. initiation, growth and interaction of fractures**
Int J Rock Mech Min Sci Geomech Abstr, 27 (5) (1990), pp. 409-427
ArticleDownload PDFView Record in Scopus

20

B. Haimson, H. Lee**Borehole breakouts and compaction bands in two high-porosity sandstones**
Int J Rock Mech Min Sci, 41 (2) (2004), pp. 287-301
ArticleDownload PDFView Record in Scopus

21

B. Haimson**Micromechanisms of borehole instability leading to breakouts in rocks**
Int J Rock Mech Min Sci, 44 (2007), pp. 157-173
ArticleDownload PDFView Record in Scopus

22

A.A. Griffith**The phenomena of rupture and flow in solids**
Philos Trans R Soc Lond A: Math, Phys Eng Sci, 221 (582–593) (1921), pp. 163-198

CrossRefView Record in Scopus

23

G.R. Irwin**Analysis of stresses and strains near the end of a crack**
J Appl Mech, 24 (1957), pp. 361-364
View Record in Scopus

24

G.I. Barenblatt**The mathematical theory of equilibrium cracks in brittle fracture**
H.L. Dryden, Th von Kármán, G. Kuerti, F.H. van den Dungen, L. Howarth (Eds.), Advances in Applied Mechanics, Elsevier (1962), pp. 55-129
ArticleDownload PDFView Record in Scopus

25

M. Kachanov, E.L.E. Montagut, J.P. Laures**Mechanics of crack—microcrack interactions**
Mech Mater, 10 (1–2) (1990), pp. 59-71
ArticleDownload PDFView Record in Scopus

26

M.J. Heap, D.R. Faulkner, P.G. Meredith, S. Vinciguerra**Elastic moduli evolution and accompanying stress changes with increasing crack damage: implication for stress change around fault zones and volcanoes during deformation**
Geophys J Int, 183 (2010), pp. 225-236
CrossRefView Record in Scopus

27

F. Erdogan**Fracture mechanics**
Int J Solids Struct, 37 (1–2) (2000), pp. 171-183
ArticleDownload PDFView Record in Scopus

28

Z. Reches, D.A. Lockner**Nucleation and growth of faults in brittle rocks**
J Geophys Res: Solid Earth, 99 (B9) (1994), pp. 18159-18173
CrossRef

29

O. Katz, Z. Reches**Microfracturing damage, and failure of brittle granites**
J Geophys Res: Solid Earth, 109 (B1) (2004), p. B01206
View Record in Scopus

30

M.J. Heap, D.R. Faulkner**Quantifying the evolution of static elastic properties as crystalline rock approaches failure**
Int J Rock Mech Min Sci, 45 (2008), pp. 564-573
ArticleDownload PDFView Record in Scopus

31

N. Moës, T. Belytschko**Extended finite element method for cohesive crack growth**

Eng Fract Mech, 69 (7) (2002), pp. 813-833
ArticleDownload PDFView Record in Scopus

32

J. Lemaitre**How to use damage mechanics**
Nucl Eng Des, 80 (1984), pp. 233-245
ArticleDownload PDFView Record in Scopus

33

J. Mazars, G. Pijaudier-Cabot**From damage to fracture mechanics and conversely: a combined approach**
Int J Solids Struct, 33 (20) (1996), pp. 3327-3342
ArticleDownload PDFView Record in Scopus

34

J. Mazars**A description of micro- and macroscale damage of concrete structures**
Eng Fract Mech, 25 (5) (1986), pp. 729-737
ArticleDownload PDFView Record in Scopus

35

Simulia. *Concrete Damaged Plasticity*. Rode Islan; 2015.

36

L. Jing**A review of techniques, advances and outstanding issues in numerical modelling for rock mechanics and rock engineering**
Int J Rock Mech Min Sci, 40 (3) (2003), pp. 283-353
ArticleDownload PDFView Record in Scopus

37

L. Jing, J.A. Hudson**Numerical methods in rock mechanics**
Int J Rock Mech Min Sci, 39 (4) (2002), pp. 409-427
ArticleDownload PDFView Record in Scopus

38

G. Kirsch**Die Theorie der Elastizit¨at und die Bedurfnisse der Festigkeitslehre**
Z Des Ver Dtsch Ing, 42 (1898), pp. 797-807

39

Z. Bazant, T. Belytschko, T. Chang**Continuum theory for strain-softening**
J Eng Mech, 110 (12) (1984), pp. 1666-1692
CrossRefView Record in Scopus

40

M.D. Zoback, D. Moos, L. Mastin, R.N. Anderson**Wellbore breakouts and in situ stress**
J Geophys Res, 90 (1985), pp. 5523-5530
CrossRefView Record in Scopus

41

B. Shen, O. Stephansson, M. Rinne**Simulation of Borehole Breakouts using FRACOD2d**

Oil Gas Sci Technol, 57 (2002), pp. 579-590
CrossRefView Record in Scopus

42

E. Eberhardt, D. Stead, B. Stimpson**Quantifying progressive pre-peak brittle fracture damage in rock during uniaxial compression**
Int J Rock Mech Min Sci, 36 (3) (1999), pp. 361-380
ArticleDownload PDFView Record in Scopus

43

D.R. Faulkner, T.M. Mitchell, D. Healy, M.J. Heap**Slip on 'weak' faults by the rotation of regional stress in the fracture damage zone**
Nature, 444 (2006), pp. 922-925
CrossRefView Record in Scopus

44

S. Busetti, K. Mish, P. Hennings, Z. Reches**Damage and plastic deformation of reservoir rocks: Part 2. Propagation of a hydraulic fracture**
AAPG Bull, 96 (9) (2012), pp. 1711-1732
CrossRefView Record in Scopus

45

I. Borg, J. Handin**Experimental deformation of crystalline rocks**
Tectonophysics, 3 (4) (1966), pp. 249-367
ArticleDownload PDFView Record in Scopus

46

A. Hillerborg, M. Modéer, P.E. Petersson**Analysis of crack formation and crack growth in concrete by means of fracture mechanics and finite elements**
Cem Concr Res, 6 (6) (1976), pp. 773-781
ArticleDownload PDFView Record in Scopus